GPS Solutions (2019) 23:46
https://doi.org/10.1007/s10291-019-0839-x

GPS ON THE WEB

Open-source MATLAB code for GPS vector tracking on a software-defined receiver

Bing Xu[1] · **Li-Ta Hsu**[1]

Abstract

The research regarding global positioning system (GPS) vector tracking (VT), based on a software-defined receiver (SDR), has been increasing in recent years. The strengths of VT include its immunity to signal interference, its capability to mitigate multipath effects in urban areas, and its excellent performance in tracking signals under high-dynamic applications. We developed open-source MATLAB code for GPS VT SDR to enable researchers and scientists to investigate its pros and cons in various applications and under various environments. To achieve this goal, we developed an "equivalent conventional tracking (CT)" SDR as a baseline to compare with VT. The GPS positioning estimator of this equivalent CT is based on an extended Kalman filter (EKF), which has exactly the same state, system, and carrier measurement models and noise tuning method as VT. This baseline provides users with a tool to compare the performance of VT and CT on common ground. In addition, this MATLAB code is well organized and easy to use. Users can quickly implement and evaluate their own newly developed baseband signal processing algorithms related to VT. The implementation of this VT code is described in detail. Finally, static and kinematic experiments were conducted in an urban and open-sky area, respectively, to show the usage and performance of the developed open-source GPS VT SDR.

Keywords GPS · Software-defined receiver (SDR) · Vector tracking (VT) · Open-source software · Extended Kalman filter (EKF)

Introduction

Reliable navigation is highly desirable in challenging environments where navigation satellite signals are interfered with and attenuated. To obtain a navigation solution, satellite signals must be tracked continually, so that the ephemeris data can be decoded and the measurements (such as pseudoranges and pseudorange rates) can be extracted. In the conventional global positioning system (GPS) receivers, each acquired satellite is allocated to an individual tracking channel. Each channel has two closed loops: one for code and one for carrier. All tracking channels are independent of each other, i.e., there are no interaction between channels and no information exchange between signal tracking and navigation processors. In vector tracking (VT)-based receivers, tracking channels are coupled together through the navigation processor, often based on an extended Kalman filter (EKF). Different forms of Kalman filter implementation can be found in (Won et al. 2010). The fundamental principle behind VT is the relationship between the code or carrier phase and the receiver states of position, velocity and time (PVT), which was first proposed by Copps in the early 1980s (Copps et al. 1980). The vector delay lock loop (VDLL) is described in (Spilker 1996), where the code is tracked in the vector mode, while the carrier tracking remains the same as in the conventional receiver. The boom of computer technologies and inertial devices has pushed the development and application of vector tracking in the last 2 decades.

The previous research has mainly focused on the advantages of vector tracking over the conventional tracking. The most commonly cited benefits are its increased capabilities in harsh environments, e.g., low carrier-to-noise ratio (CNR) (Lashley and Bevly 2009; Lashley et al. 2009; Pany and Eissfeller 2006), intermittent signal outages (Lashley and Bevly 2007; Zhao and Akos 2011; Zhao et al. 2011), and high dynamics (Lashley et al. 2009), due to the

✉ Li-Ta Hsu
lt.hsu@polyu.edu.hk

[1] Interdisciplinary Division of Aeronautical and Aviation Engineering, The Hong Kong Polytechnic University, Kowloon, Hong Kong

Published online: 05 March 2019

mutual aiding of the channels with respect to each other and a higher filtering gain to be used stably (Groves and Mather 2010). To further improve robustness and accuracy in poor environments, vector tracking can be easily integrated with an inertial navigation system (INS) by simply augmenting the navigation Kalman filter with appropriate INS-related states (Lashley and Bevly 2013; Luo et al. 2012; Petovello and Lachapelle 2006). In recent years, with the increasing development of intelligent transportation systems and location-based services in urban canyon areas, vector tracking has received more attention. For example, in (Hsu et al. 2013, 2015; Syed Dardin et al. 2013), vector tracking is applied to multipath or non-line-of-sight reception mitigation in the signal processing stage, while, in (Ng and Gao 2017), deeply coupled multi-receiver vector tracking is used to improve the reliability and robustness of GPS signal tracking and position estimation. A more recent paper converts a software-defined receiver (SDR) to a signal simulator using vector tracking loop to create desired line-of-sight parameters for updating the numerically controlled oscillator (NCO) and, therefore, generate the code and carrier replicas (Maier et al. 2018). Apart from the benefits and applications mentioned above, vector tracking has also been used to improve bit synchronization and decoding (Ren et al. 2013), estimate ionosphere residual error (Shytermeja et al. 2017), enhance carrier phase tracking (Brewer and Raquet 2016), etc. The idea of vector tracking also yields the other signal tracking techniques, e.g., direct position tracking loops (Liu et al. 2011) and robust adaptive joint tracking (Tabatabaei and Mosavi 2017). It should be noted that the coupling of loops is not only responsible for vector tracking's superior performance, but also allows error propagation among loops, which has been dealt with in (Bhattacharyya and Gebre-Egziabher 2010; Sun et al. 2017).

The majority of the current research generally focuses on the exploration of benefits offered by vector tracking, but seldom presents the detailed implementation of vector tracking. In 2011, Zhao and Akos (Zhao and Akos 2011) published an open-source code of vector tracking based on the GPS software-defined receiver developed by Borre et al. (2007), which is a popular open-source SDR platform for beginners. In Zhao's open-source software, the performance of vector tracking is compared with that of traditional scalar loops and navigation solutions estimated using the least-squares method. In fact, improvements of vector tracking might be due to the Kalman filter; an equivalent conventional receiver must be implemented as a reference. In this paper, a fully self-developed SDR based on vector tracking is presented. An equivalent conventional tracking (CT)-based SDR using delay lock loop (DLL) and phase lock loop (PLL) is also implemented for performance comparison between VT and CT. The CT-based SDR uses an EKF to estimate receiver's PVT. The system propagation and measurement model and the noise tuning method are exactly the same for VT and CT. This feature can bring them both to common ground to allow an accurate performance evaluation.

In the following sections, the design of vector tracking in the open-source SDR is described first. Afterward, main functionalities of the software are given. Then, the experiments are conducted to evaluate the performance of this software. Finally, conclusions are drawn, including future work.

Vector tracking algorithm

In this SDR, VDLL is implemented as an example. Users can easily extend this software to vector frequency lock loop (VFLL), or vector delay/frequency lock loop (VDFLL). Figure 1 presents the architecture of this SDR. As shown in Fig. 1,

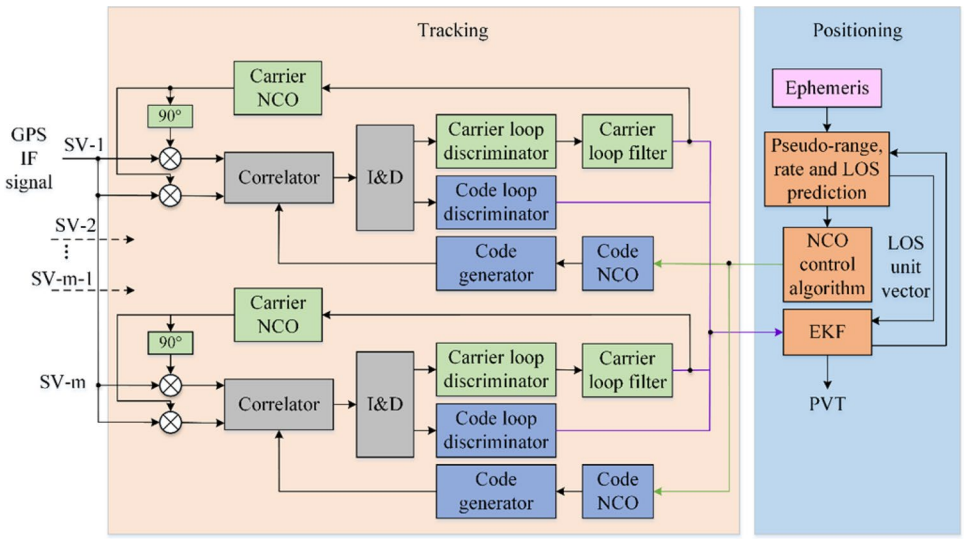

Fig. 1 The tracking architecture of the developed GPS VT SDR

each acquired satellite in the incoming intermediate frequency (IF) signal is allocated to one tracking channel. In each channel, IF signals are first multiplied with the locally generated carrier replica in both in-phase and quadrature arms. Correlation is then performed between the code replicas and the received ones. In this paper, three code replicas spacing of 0.5 chips are generated. Afterwards, correlation results are integrated and dumped. The output of these integrations is used as the input to the carrier/code loop discriminator to find the phase error of the local carrier and code replicas. In each carrier loop, the carrier discriminator output is filtered and fed back to the carrier NCO, so as to modify the frequency of local carrier replica. For the code tracking loop, code discriminator outputs of all channels are forwarded to the navigation processor. In this paper, an EKF is used. The output of the carrier loop filter, i.e., Doppler shift frequency information, is also fed into the EKF. Note that, in practice, the EKF update time is not necessary to be the same as the coherent integration time (typically 1 ms for GPS L1 signal). A pre-filter can be used to average the code discriminator outputs over multiple integration time, e.g., 20 ms.

The EKF estimates the receiver PVT based on its system propagation and the measurements, which will be described in detail later. After obtaining the navigation solution, the pseudorange and its rate and the line-of-sight (LOS) vector between the receiver and the satellites are predicted. To do this, the satellite ephemeris data must be known a priori. In this paper, the conventional tracking is used to process the IF signal and decode the ephemeris data first. The PVT calculated using the conventional tracking is then used to initialize the VDLL. Finally, the predicted pseudoranges are used to control the code NCO and then are fed back to each channel.

Design of the extended Kalman filter

The state vector of the EKF is as follows:

$$\boldsymbol{X} = \left[\Delta p_x, \Delta p_y, \Delta p_z, \Delta v_x, \Delta v_y, \Delta v_z, \Delta b, \Delta d\right]^T, \tag{1}$$

where $\Delta\boldsymbol{p} = \left[\Delta p_x, \Delta p_y, \Delta p_z\right]$ and $\Delta\boldsymbol{v} = \left[\Delta v_x, \Delta v_y, \Delta v_z\right]$ are the three-dimensional receiver position and velocity error vectors in an earth-centered and earth-fixed (ECEF) frame; Δb and Δd are the receiver clock bias and drift errors in the units of meters and meters per second, respectively. The system propagation at epoch k is as follows:

$$\hat{\boldsymbol{X}}_k^- = \boldsymbol{\Phi}_{k-1}\hat{\boldsymbol{X}}_{k-1}^+, \tag{2}$$

where

$$\boldsymbol{\Phi}_{k-1} = \begin{bmatrix} \boldsymbol{I}_{3\times3} & \boldsymbol{\tau I}_{3\times3} & 0_{3\times2} \\ 0_{3\times3} & \boldsymbol{I}_{3\times3} & 0_{3\times2} \\ 0_{2\times3} & 0_{2\times3} & \boldsymbol{K} \end{bmatrix}_{8\times8} \tag{3}$$

$$\boldsymbol{K} = \begin{bmatrix} 1 & \tau \\ 0 & 1 \end{bmatrix}. \tag{4}$$

In Eq. (3), τ is the update interval of the EKF. The superscript and subscript, "−" and "+", denote the system state before and after measurement update, respectively. The symbol "^" represents the EKF estimates.

The measurements of the EKF are the pseudorange error, $\Delta\rho^j$, and pseudorange rate error, $\Delta\dot{\rho}^j$, of satellite j. The pseudorange error is as follows:

$$\Delta\rho^j = \Delta\tau^j \cdot \frac{c}{f_{\mathrm{CA}}}, \tag{5}$$

where $\Delta\tau^j$ is the code discriminator output in chips, f_{CA} is the code chipping rate (1.023 MHz for GPS L1 C/A); c is the speed of light. The error of pseudorange rate is the difference between the measured pseudorange rates extracted from the carrier tracking loop and the predicted ones calculated using the estimated receiver velocity and satellite velocity as well as the estimated receiver clock drift:

$$\Delta\dot{\rho}^j = f^j_{\mathrm{Doppler}} \cdot \frac{c}{f_{\mathrm{L1}}} - \left(\boldsymbol{v}_{\mathrm{usr}} - \boldsymbol{v}^j_{\mathrm{sate}}\right) \cdot \boldsymbol{l}^j - \hat{d}_{u,\mathrm{clk}} + d^j_{\mathrm{sv,clk}}, \tag{6}$$

where f^j_{Doppler} is the Doppler shift frequency in Hz; f_{L1} is the carrier frequency (1575.42 MHz for GPS L1); $\boldsymbol{v}_{\mathrm{usr}}$ and $\boldsymbol{v}^j_{\mathrm{sate}}$ are the velocity vectors of the receiver and satellite j, respectively; $\boldsymbol{l}^j$ is the LOS unit vector from the receiver to satellite j; $\hat{d}_{u,\mathrm{clk}}$ and $d^j_{\mathrm{sv,clk}}$ are the estimated receiver clock drift and the jth satellite clock drift, respectively, both in meters per second. The measurement vector can be expressed as follows:

$$\boldsymbol{Z} = \left[\Delta\rho^1, \Delta\rho^2, \cdots, \Delta\rho^m,\ \Delta\dot{\rho}^1, \Delta\dot{\rho}^2, \cdots, \Delta\dot{\rho}^m\right]^T. \tag{7}$$

where m is the number of satellites involved in positioning. The relationship between the state vector and the measurement vector at epoch k is linearized by a first-order Taylor's expression as follows:

$$\boldsymbol{Z}_k = \boldsymbol{H}_k \cdot \boldsymbol{X}_k, \tag{8}$$

where $\boldsymbol{H}$ is the measurement matrix, calculated as follows:

$$\boldsymbol{H} = \begin{bmatrix} -\boldsymbol{l}^1_x & -\boldsymbol{l}^1_y & -\boldsymbol{l}^1_z & 0 & 0 & 0 & 1 & 0 \\ -\boldsymbol{l}^2_x & -\boldsymbol{l}^2_y & -\boldsymbol{l}^2_z & 0 & 0 & 0 & 1 & 0 \\ \vdots & \vdots & \vdots & \vdots & \vdots & \vdots & \vdots & \vdots \\ -\boldsymbol{l}^m_x & -\boldsymbol{l}^m_y & -\boldsymbol{l}^m_z & 0 & 0 & 0 & 1 & 0 \\ 0 & 0 & 0 & -\boldsymbol{l}^1_x & -\boldsymbol{l}^1_y & -\boldsymbol{l}^1_z & 0 & 1 \\ 0 & 0 & 0 & -\boldsymbol{l}^2_x & -\boldsymbol{l}^2_y & -\boldsymbol{l}^2_z & 0 & 1 \\ \vdots & \vdots & \vdots & \vdots & \vdots & \vdots & \vdots & \vdots \\ 0 & 0 & 0 & -\boldsymbol{l}^m_x & -\boldsymbol{l}^m_y & -\boldsymbol{l}^m_z & 0 & 1 \end{bmatrix}, \tag{9}$$

The subscript of the LOS unit vector denotes its x, y, and z components, and the superscript denotes the satellite.

Noise tuning of the EKF

The process noise comes from two sources, i.e., the receiver dynamics and clock noise, as follows:

$$\boldsymbol{Q} = \begin{bmatrix} \boldsymbol{Q}_{\text{dyn}} & 0_{6\times2} \\ 0_{2\times6} & \boldsymbol{Q}_{\text{clk}} \end{bmatrix}. \tag{10}$$

The values of $\boldsymbol{Q}_{\text{dyn}}$ and $\boldsymbol{Q}_{\text{clk}}$ can be set empirically according to the receiver motion state and the oscillator used. Alternatively, they can be calculated as follows:

$$\boldsymbol{Q}_{\text{dyn}} = \begin{bmatrix} \tau^3/3 \cdot \boldsymbol{I}_{3\times3} & \tau^2/2 \cdot \boldsymbol{I}_{3\times3} \\ \tau^2/2 \cdot \boldsymbol{I}_{3\times3} & \tau \cdot \boldsymbol{I}_{3\times3} \end{bmatrix} \cdot S_{\text{v}} \tag{11}$$

$$\boldsymbol{Q}_{\text{clk}} = \begin{bmatrix} S_{\text{f}} \cdot \tau + S_{\text{g}}\tau^3/3 & S_{\text{g}}\tau^2/2 \\ S_{\text{g}}\tau^2/2 & S_{\text{g}} \cdot \tau \end{bmatrix}, \tag{12}$$

where S_{v} is the receiver velocity noise power spectral density (PSD); S_{f} andS_{g} are the PSD of receiver clock phase and frequency, respectively. The value of S_{v} should be set according to the level of dynamics. Settings of S_{f} and S_{g} are usually based on the rule of thumb values of the type of oscillator used, or calculated using the following formulas:

$$S_{\text{f}} = c^2 \cdot \frac{h_0}{2} \tag{13}$$

$$S_{\text{g}} = c^2 \cdot 2\pi^2 \cdot h_{-2}, \tag{14}$$

where h_0 and h_{-2} are the coefficients of white frequency modulation noise and flicker frequency modulation noise of the oscillator used, respectively.

The measurement noise covariance matrix is calculated adaptively using the innovation-based adaptive estimation technique (Mohamed and Schwarz 1999). The measurement innovation at epoch $k+1$ in this paper is as follows:

$$\boldsymbol{V}_{k+1} = \boldsymbol{Z}_{k+1} - \boldsymbol{Z}_{k+1}^{-} \tag{15}$$

$$\boldsymbol{Z}_{k}^{-} = \boldsymbol{H}_k \hat{\boldsymbol{X}}_k^{-}. \tag{16}$$

The diagonal element of the measurement covariance matrix is the variance of the measurement innovation. The off-diagonal terms are assumed to be zero due to the weak correlation between channels.

Main functionalities of the open-source SDR

This open-source SDR is developed using MATLAB, which is an easy-to-use programming language, so that users can focus more on the implementation of the newly developed algorithms. Figure 2 presents the flowchart of the software. The four main functionalities include initialization, acquisition, conventional tracking, and vector tracking, which are described in detail as follows:

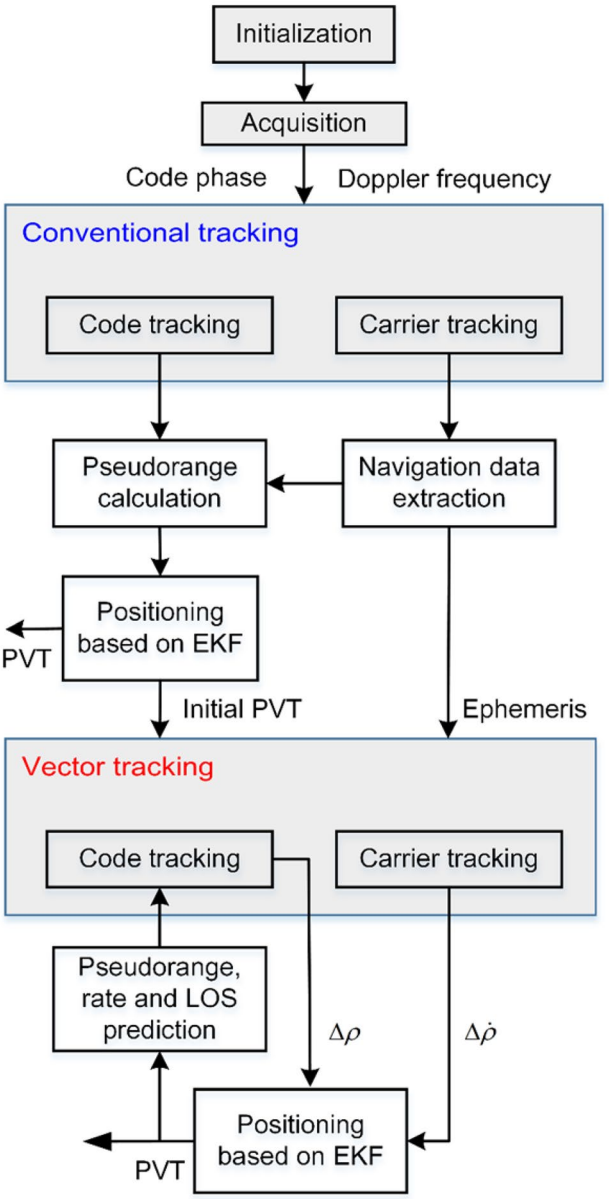

Fig. 2 Flowchart of the open-source GPS SDR

Initialization

The first step to use this software is to complete configurations such as the sampling rate and intermediate frequency of the raw signal, the frequency step, and band to be searched in the acquisition, etc.

Acquisition

The second module is signal acquisition, which determines code phase and Doppler frequency of visible satellites. A two-step coarse-to-fine acquisition method is used. In the first step, 4-ms data are used to detect the code phase and Doppler frequency coarsely via the parallel code phase search acquisition algorithm (Van Nee and Coenen 1991). The second step utilizes long C/A code-stripped data to find the carrier frequency accurately via the fast Fourier transformation technique.

Conventional tracking

After obtaining the code phase and Doppler frequency, these two parameters should be refined in the tracking stage, so that satellite ephemeris data can be decoded. Measurements of pseudorange and pseudorange rate can also be obtained during tracking. A second-order DLL and PLL is used in this software. With this information, the navigation solution is calculated in the positioning module, which is based on an EKF instead of the least-squares method in this SDR, because any improvements of vector tracking might be due to the Kalman filter. The EKF used in the conventional receiver has the same states, system, and measurement models as the vector tracking EKF. The noise tuning of these two EKFs is also the same so as to compare the performance of the conventional and vector tracking methods based on common ground. Even so, there still exist two differences between the conventional tracking and vector tracking. One difference is the formation of pseudorange error measurements. In the conventional tracking, it is calculated by the measured pseudorange minus the predicted pseudorange as follows:

$$\Delta\rho^j = c\left(t_{rx} - t_{tx}^j\right) - \left\|\boldsymbol{r}_u - \boldsymbol{r}^j\right\| - \hat{b}_{\text{clk}}, \tag{17}$$

where t_{rx} is the receiver time in a conventional receiver; t_{tx}^j is the transmission time from satellite j; $\boldsymbol{r}_u$ and $\boldsymbol{r}^j$ are the position of receiver and satellite j, respectively; $\hat{b}_{\text{clk}}$ is the estimated receiver clock bias. In vector tracing, however, the pseudorange error is calculated, as shown in (5). The other difference is the operating mode of the code tracking loop. In the conventional tracking, all code tracking channels are independent closed loops. The feedback to the code NCO is the code discriminator output in each channel. However, in vector tracking, the feedback is calculated using the estimated navigation solution as follows:

$$f_{\text{code},k+1}^j = f_{\text{CA}}\left[1 - \frac{\tilde{\rho}_{k+1}^j - \hat{\rho}_k^j}{c\tau}\right], \tag{18}$$

where $\tilde{\rho}_{k+1}^j$ and $\hat{\rho}_k^j$ are the predicted pseudorange at epoch $k+1$ and the estimated pseudorange at epoch k. The predicted pseudorange is calculated using the following:

$$\tilde{\rho}_{k+1}^j = \left\|\tilde{\boldsymbol{r}}_{u,k+1} - \boldsymbol{r}_{k+1}^j\right\| + \delta\hat{\rho}_{\text{sv},c}^j + \delta\hat{\rho}_I^j + \delta\hat{\rho}_T^j - \hat{b}_{\text{clk}}, \tag{19}$$

where $\boldsymbol{r}_{k+1}^j$ and $\tilde{\boldsymbol{r}}_{u,k+1}$ are the satellite position and the predicted receiver position at epoch $k+1$, respectively. $\boldsymbol{r}_{k+1}^j$ is known from the broadcast ephemeris, while $\tilde{\boldsymbol{r}}_{u,k+1}$ can be calculated based on the estimated position and clock bias at the previous epoch. $\delta\hat{\rho}_{sv,c}^j$, $\delta\hat{\rho}_I^j$, and $\delta\hat{\rho}_T^j$ are the pseudorange errors caused by satellite clock error, ionospheric delay, and tropospheric delay, respectively. $f_{\text{code},k+1}^j$ is then fed back to the code NCO in each channel to generate local code replicas.

Vector tracking

To start vector tracking, initialization parameters, such as ephemeris data, initial receiver PVT, etc., should be provided. The pseudorange error, $\Delta\rho$, and pseudorange rate error, $\Delta\dot{\rho}$, extracted from the code and carrier tracking loops are used as the measurements of the EKF. The estimated receiver PVT is then used to predict the pseudorange, rate, and the LOS vectors at the next epoch.

Experiments and results

Two experimental tests were conducted to evaluate the performance of vector tracking in terms of its ability against multipath and dynamics effects, respectively. In the first test, signals were collected statically in an urban area of Hong Kong, as shown in Fig. 3a. It is expected that the positioning accuracy would decrease due to the potential multipath effects. The second test was conducted in an open-sky environment. In this test, the antenna was mounted on the roof of an automobile which kept static for about 30 s before moving with a moderate dynamic along a coast, as shown in Fig. 3b. A geodetic-grade receiver, NovAtel Flexpak6, was used to provide a reference trajectory. The experimental setup of the kinematic test is shown in Fig. 3c. In both tests, GPS signals were collected using a Nottingham Scientific Ltd. (NSL) Stereo front-end for postprocessing by the developed software. The sampling frequency and IF of the front-end are 26 MHz and 6.5 MHz, respectively. In both tests, the update

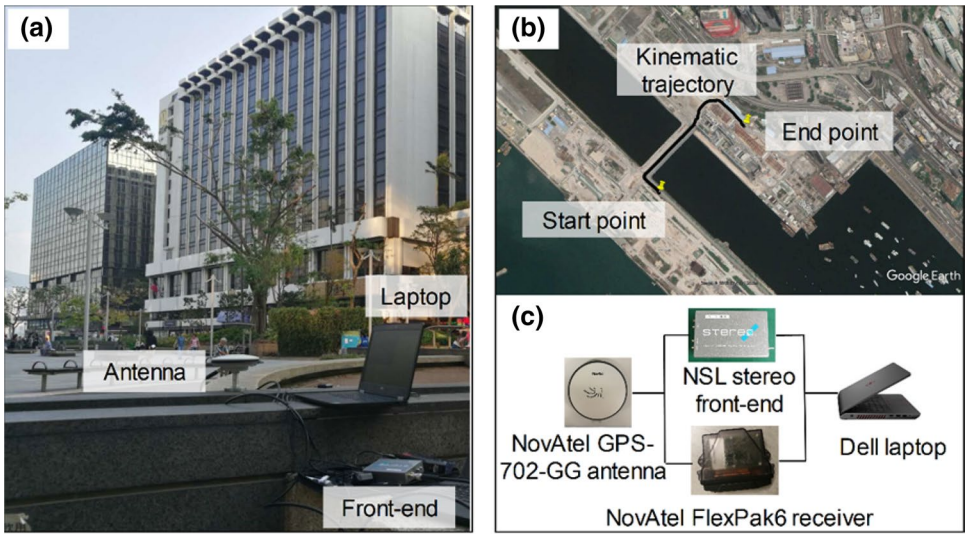

Fig. 3 Experimental environments and setup

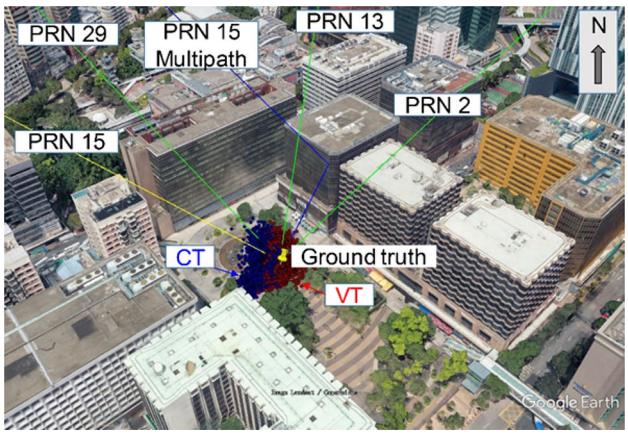

Fig. 4 Positioning results and ray tracing results of the four trackable GPS satellites

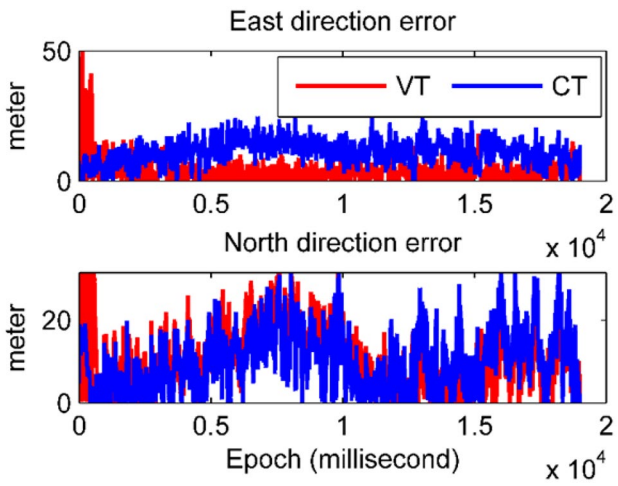

Fig. 5 Positioning errors in east and north direction

interval of the EKF is 1 ms. The process noise covariance matrix is a diagonal matrix, with its main diagonal values set empirically as diag[0.2, 0.2, 0.2, 0.1, 0.1, 0.1, 0.1, 0.01]. Here, diag[·] denotes a diagonal matrix. The measurement noise is calculated adaptively using Eqs. (15) and (16).

Static test results

In this test, the receiver antenna was surrounded by high buildings. Only four GPS satellites (PRN 2, 13, 15, and 29) can be acquired and tracked continually using the software receiver, as shown in Fig. 4. Figure 4 also shows the ray tracing (Hsu et al. 2016) results of these four satellites based on the ground truth position, among which PRN 15 is a multipath signal, with its direct and reflected signal paths marked in yellow and blue, respectively.

Figure 5 presents the positioning errors in east and north directions of vector tracking and conventional tracking during about 20 s. The conventional tracking exhibits a mean offset of 11.29 m in the east direction, while vector tracking remains a lower mean positioning error of 4.19 m. In north direction, the two methods have similar performance, with a mean error of 10.26 m and 10.89 m for vector tracking and conventional tracking, respectively.

The positioning offset is probably due to the multipath effect from PRN 15. The mechanism by which the vector tracking outperforms the convention tracking in terms of multipath mitigation can be seen in Fig. 6, which demonstrates the code discriminator output and code frequency of PRN 15. Even though the code discriminator output of vector tracking is noisy, the code frequency which directly determines the local code replica generation is slightly more stable for vector tracking. This improvement is due to the fact that the code frequency is calculated not only from the measurements but also using the system propagation model.

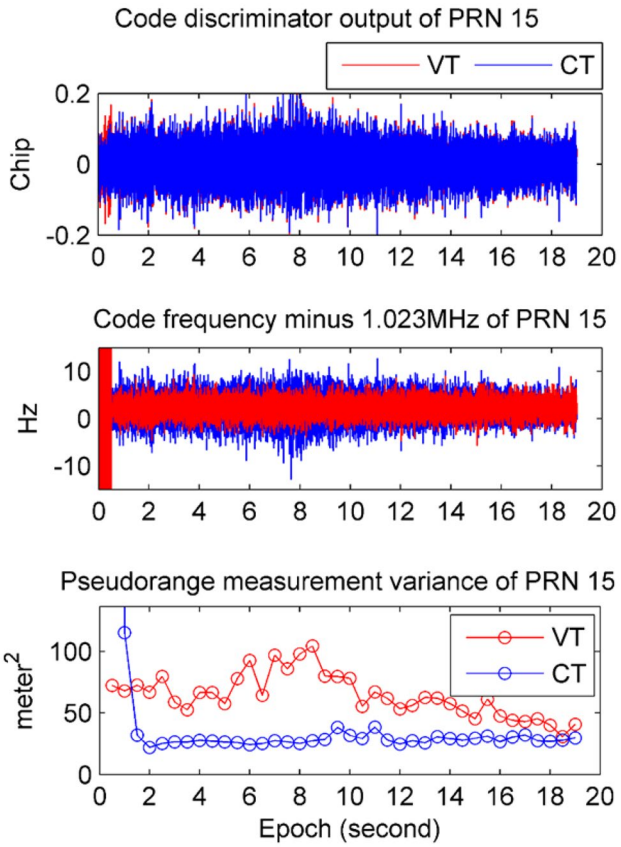

Fig. 6 Code discriminator output, code frequency, and pseudorange measurement variance of PRN 15

The bottom of Fig. 6 shows the pseudorange measurement variance of PRN 15. Vectoring tracking reports a larger measurement variance during the whole test, which indicates that the measurement of PRN 15 contributes less in positioning.

Kinematic test results

Figure 7 shows the kinematic positioning results of vector tracking, conventional tracking, and NovAtel receiver in a Google map. The U-shape trajectory contains two right turns, a quarter turn and a round turn with a radius of about 40 m.

The NovAtel Flexpak6 is a dual-frequency plus L-Band GNSS receiver, and thus, it has the best positioning result, which is used as the reference for evaluating the other two methods. As seen from Fig. 7, both vector tracking and conventional tracking perform well in the static stage. However, the conventional tracking has a large positioning error near the round turn. This is due to the signal tracking failure caused by the automobile dynamics, which can be confirmed in Fig. 8. As can be seen in upper panel of Fig. 8, at around 50 s, the CNR of PRN 31 suffers a sudden

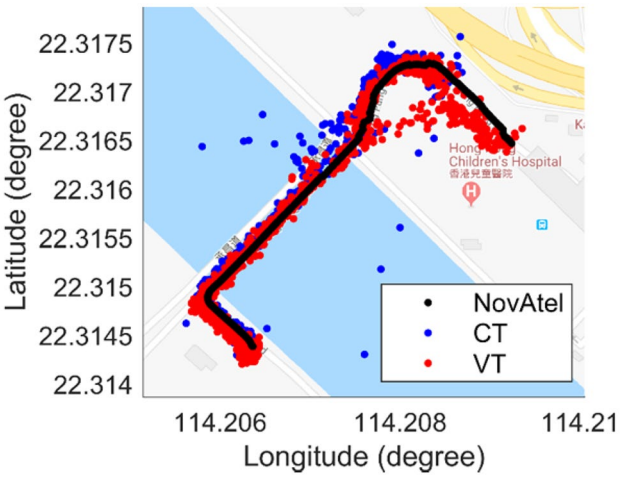

Fig. 7 Positioning results in the kinematic test in an open-sky area plotted in a Google map

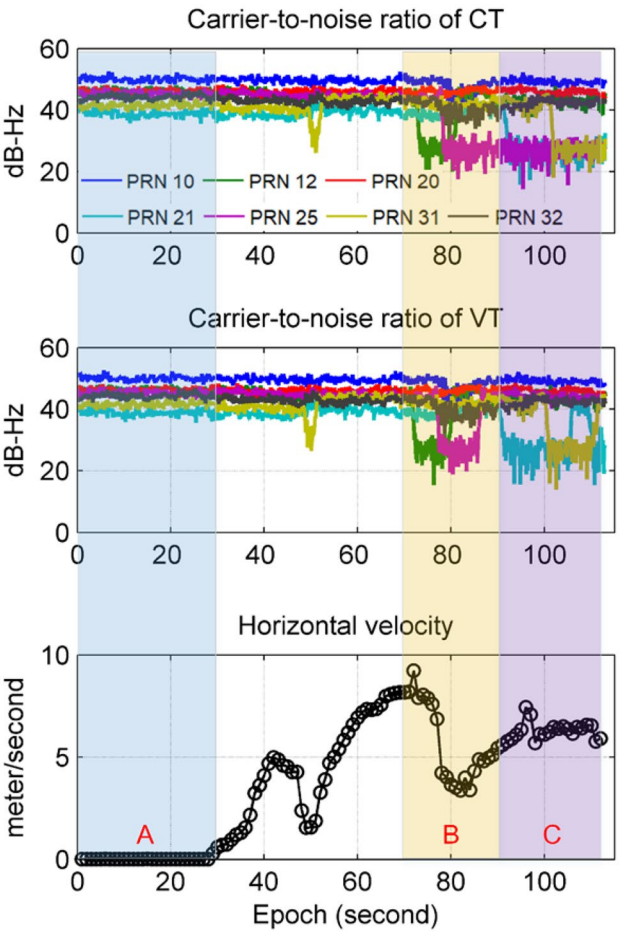

Fig. 8 Carrier-to-noise ratio of vector tracking and conventional tracking, and the horizontal velocity during the kinematic test

decrease. About 2 s later, the value returns to the regular level, which indicates that the tracking loop of PRN 31 relocks onto this signal. PRN 12 also suffers from this problem at around 75 s (Period B in the vertical yellow shadow), but it takes more time to recover. After that, the CNR values of PRNs 25, 21, and 31 decrease successively (Period C in purple shadow). Unfortunately, these tracking loops never relock onto the lost signals. Looking at the lower part of Fig. 8, the velocity values have a high correlation with the CNR values, which means that the decrease of CNR is caused by the automobile dynamics. The middle panel in Fig. 8 is the CNR of vector tracking. Compared with that of conventional tracking, vector tracking also suffers from the automobile dynamics, but after a period of time, the lost signals (PRNs 31, 12, 25, and 21) can be relocked in vector tracking. This is because the code frequency of the lost signal can be predicted using the navigation solution calculated using the information of other channels in vector tracking. In Fig. 8, the static stage is marked in light blue shadow, Period A.

The horizontal positioning errors of conventional tracking and vector tracking are presented in Fig. 9. The detailed quantitative positioning errors are listed in Table 1. It can be seen that, in the static stage, the two methods have similar performances. However, in the kinematic process, vector tracking has a lower positioning error than the conventional tracking, especially after 50 s when the automobile is in acceleration and deceleration processes.

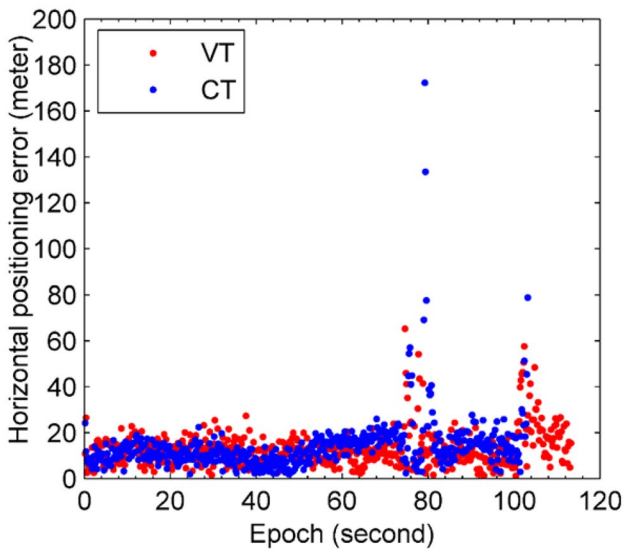

Fig. 9 Horizontal positioning error of vectoring tracking and conventional tracking. The reference trajectory is provided by NovAtel Flexpak6 receiver

Table 1 Horizontal positioning errors in three selected periods

Period (second)	Error (meter)	
	CT	VT
Static period		
A (1–30)	10.79	11.70
Kinematic period		
B (70–90)	21.14	14.31
C (91–113)	679.89	16.19

Conclusions

A GPS SDR based on vector tracking is implemented in this paper. The algorithm design of vector delay lock loop is presented, with an emphasis on the design of the EKF. A conventional tracking-based receiver is also developed, which calculates the receiver navigation solution using the same EKF as vectoring tracking. Static and kinematic tests are conducted in an urban area and an open-sky environment, respectively, to evaluate the performance of vectoring tracking and conventional tracking. Results show that vector tracking has a better capability against signal interference, e.g., multipath signal. Besides, in terms of dynamic performance, vector tracking outperforms the conventional tracking due to its coupling of all the tracking channels.

The open-source GPS SDR can be used as a basic tool to learn the principle of vector tracking and compare its performance with the conventional tracking. The contents and functionalities of this software will be continually improved. The current MATLAB software can be found on the GPS Toolbox website at: https://www.ngs.noaa.gov/gps-toolbox. A user manual is also provided, which shows how to install the software and how to process the data collected using a front-end. Any comments, suggestions, or corrections are welcome; please send these to the authors.

Acknowledgements The authors acknowledge the support of Hong Kong PolyU startup fund on the project 1-ZVKZ, "Navigation for Autonomous Driving Vehicle using Sensor Integration".

References

Bhattacharyya S, Gebre-Egziabher D (2010) Development and validation of parametric models for vector tracking loops. Navig J Inst Navig 57:275–295

Borre K, Akos D, Bertelsen N, Rinder P, Jensen S (2007) A software defined GPS and Galileo receiver—a single-frequency approach. Applied and numerical harmonic analysis, Birkhäuser, Boston

Brewer J, Raquet J (2016) Differential vector phase locked loop. IEEE Trans Aerosp Electron Syst 52:1046–1055

Copps E, Geier G, Fidler W, Grundy P (1980) Optimal processing of GPS signals. Navig J Inst Navig 27:171–182

Groves P, Mather C (2010) Receiver interface requirements for deep INS/GNSS integration and vector tracking. J Navig 63:471–489

Hsu L-T, Groves P, Jan S (2013) Assessment of the multipath mitigation effect of vector tracking in an urban environment. In: Proceedings of ION Pacific PNT 2013, Honolulu, Hawaii, 22–25 April 2013, pp 498–509

Hsu L-T, Jan S, Groves P, Kubo N (2015) Multipath mitigation and NLOS detection using vector tracking in urban environments. GPS Solut 19:249–262

Hsu L-T, Gu Y, Kamijo S (2016) 3D building model-based pedestrian positioning method using GPS/GLONASS/QZSS and its reliability calculation. GPS Solut 20:413–428

Lashley M, Bevly D (2007) Analysis of discriminator based vector tracking algorithm. In: Proceedings of ION NTM 2007, San Diego, CA, 22–24 January 2007, pp 570–576

Lashley M, Bevly D (2009) Vector delay/frequency lock loop implemenation and analysis. In: Proceedings of ION ITM 2009, Anaheim, CA, 26–28 January 2009, pp 1073–1086

Lashley M, Bevly D (2013) Performance comparison of deep integration and tight coupling. Navig J Inst Navig 60:159–178

Lashley M, Bevly DM, Hung JY (2009) Performance analysis of vector tracking algorithms for weak GPS signals in high dynamics. IEEE J Sel Top Signal Process 3:661–673

Liu J, Yin H, Cui X, Lu M, Feng Z (2011) A direct position tracking loop for GNSS receivers. In: Proceedings of ION GNSS 2011, Portland, OR, 20–23 September 2011 2011. pp 3634–3643

Luo Y, Babu R, Wu W, He X (2012) Double-filter model with modified Kalman filter for baseband signal pre-processing with application to ultra-tight GPS/INS integration. GPS Solut 16:463–476

Maier D, Frankl K, Pany T (2018) The GNSS-transceiver: using vector-tracking approach to convert a GNSS receiver to a simulator: implementation and verification for signal authentication. In: Proceedings of ION GNSS + 2018, Miami, Florida, pp 4231–4244, 24–28 September 2018

Mohamed A, Schwarz K (1999) Adaptive Kalman filtering for INS/GPS. J Geodesy 73:193–203

Ng Y, Gao GX (2017) GNSS multireceiver vector tracking. IEEE Trans Aerosp Electron Syst 53:2583–2593

Pany T, Eissfeller B (2006) Use of a vector delay lock loop receiver for GNSS signal power analysis in bad signal conditions. In: Proceedings of 2006 IEEE/ION Position, Location, And Navigation Symposium, Coronado, CA, USA, 25–27 April 2006, pp 893–903

Petovello MG, Lachapelle G (2006) Comparison of vector-based software receiver implementations with application to ultra-tight GPS/INS integration. In: Proceedings of ION GNSS 2006, Fort Worth, TX, 26–29 September 2006, pp 1790–1799

Ren T, Petovello M, Basnayake C (2013) Improving GNSS bit synchronization and decoding using vector tracking. In: Proceedings of ION GNSS + 2013, Nashville, TN, 16–20 September 2013, pp 121–134

Shytermeja E, Garcia-Pena A, Julien O (2017) Dual-constellation vector tracking algorithm in ionosphere and multipath conditions. In: Proceedings of ITSNT 2017, ENAC, Toulouse, France, 14–17 Nov 2017

Spilker JJ (1996) Fundamentals of signal tracking theory. In: Parkinson BW, Spilker JJ, Axelrad P, Enge P (eds) Global positiooning system: theory and application, vol 1. Progress in astronautics and aeronautics, vol 163, 2 edn. American Institute of Aeronautics, Washington, pp 289–327

Sun Z, Wang X, Feng S, Che H, Zhang J (2017) Design of an adaptive GPS vector tracking loop with the detection and isolation of contaminated channels. GPS Solut 21:701–713

Syed Dardin S, Calmettes V, Priot B, Tourneret J-Y (2013) Design of an adaptive vector-tracking loop for reliable positioning in harsh environment. In: Proceedings of ION GNSS + 2013, Nashville, TN, 16–20 September 2013, pp 3548–3559

Tabatabaei A, Mosavi M (2017) Robust adaptive joint tracking of GNSS signal code phases in urban canyons. IET Radar Sonar Navig 11:987–993

Van Nee D, Coenen A (1991) New fast GPS code-acquisition technique using. FFT Electron Lett 27:158–160

Won J, Dötterböck D, Eissfeller B (2010) Performance comparison of different forms of Kalman filter approaches for a vector-based GNSS signal tracking loop. Navig J Inst Navig 57:185–199

Zhao S, Akos D (2011) An open source GPS/GNSS vector tracking loop - implementation, filter tuning, and results. In: Proceedings of ION ITM 2011, San Diego, CA, 24–26 January 2011, pp 1293–1305

Zhao S, Lu M, Feng Z (2011) Implementation and performance assessment of a vector tracking method based on a software GPS receiver. J Navig 64:S151–S161

Bing Xu Bing XU is currently a Postdoctoral Fellow with Interdisciplinary Division of Aeronautical and Aviation Engineering, The Hong Kong Polytechnic University. He received his B.S. and PhD. degrees in network engineering and navigation guidance and control from Nanjing University of Science and Technology, China, in 2012 and 2018, respectively. His research focuses on signal processing in software-defined GNSS receivers.

Li-Ta Hsu Li-Ta HSU received the B.S. and Ph.D. degrees in aeronautics and astronautics from National Cheng Kung University, Taiwan, in 2007 and 2013, respectively. He is currently an assistant professor with Interdisciplinary Division of Aeronautical and Aviation Engineering, The Hong Kong Polytechnic University, before he served as post-doctoral researcher in Institute of Industrial Science at University of Tokyo, Japan. In 2012, he was a visiting scholar in University College London, UK. His research interests include GNSS positioning in challenging environment and localization for pedestrian, autonomous driving vehicle, and unmanned aerial vehicle.